Journal of
Nuclear Engineering

MDPI

Article

Mini-Reactor Proliferation-Resistant Fuel with Burnable Gadolinia in Once-Through Operation Cycle Performance Verification

John D. Bess *, Gray S. Chang, Patrick Moo and Julie Foster

JFoster & Associates, LLC, Idaho Falls, ID 83402, USA; gray.chang@gmail.com (G.S.C.); pat.moo@jfaidaho.com (P.M.); julie.foster@jfaidaho.com (J.F.)
* Correspondence: john.bess@jfaidaho.com

Abstract: A miniature nuclear reactor is desirable for deployment as a localized nuclear power station in support of a carbon-free power supply. Coupling aspects of proliferation-resistant fuel with natural burnable absorber loading are evaluated for once-through operation cycle performance to minimize the need for refueling and fuel shuffling operations. The incorporation of 0.075 wt.% ^{237}Np provides favorable plutonium isotopic vectors throughout an operational lifetime of 5.5 years. providing 35 MWe. Core performance was assessed using a verification-by-comparison approach for core designs with or without ^{237}Np and/or gadolinia burnable absorber. Burnup Monte Carlo calculations were performed via MCOS coupling of MCNP and ORIGEN to an achievable burnup of ~62.5 GWd/t. The results demonstrate a minimal penalty to reactor performance due to the addition of these materials as compared against the reference design. Coupling of a proliferation-resistant fuel concept with a uniform loading of natural gadolinia burnable absorber for LEU+ fuel (7.5 wt.% ^{235}U/U UO_2) provides favorable excess reactivity considerations with minimized concerns for additional residual waste and more uniform distribution of un-depleted ^{235}U in discharged fuel assemblies.

Keywords: LEU+; ^{237}Np; ^{238}Pu; proliferation-resistant fuel; reactor design; small modular reactor

check for updates

Citation: Bess, J.D.; Chang, G.S.; Moo, P.; Foster, J. Mini-Reactor Proliferation-Resistant Fuel with Burnable Gadolinia in Once-Through Operation Cycle Performance Verification. *J. Nucl. Eng.* **2024**, *5*, 318–329. https://doi.org/10.3390/jne5030021

Academic Editor: Dan Gabriel Cacuci

Received: 29 May 2024
Revised: 19 July 2024
Accepted: 23 July 2024
Published: 28 August 2024

Copyright: © 2024 by the authors. Licensee MDPI, Basel, Switzerland. This article is an open access article distributed under the terms and conditions of the Creative Commons Attribution (CC BY) license (https://creativecommons.org/licenses/by/4.0/).

1. Introduction

The MINI-21 is a miniature nuclear reactor design concept under development at JFoster & Associates, LLC (JFA), based upon proven pressurized water reactor (PWR) technologies implementing a 17 × 17 fuel assembly (FA) with uranium dioxide (UO_2) fuel pins. Small modular reactors (SMRs) derived using traditional PWR architecture will likely be the quickest to deployment with the lowest quantity of non-proliferation and safeguard concerns [1], and they are described as having a favorable life cycle [2]. Confirmation of overall SMR economics is however not viable until SMRs are constructed and operated [3]. The MINI-21 reactor utilizes 21 FAs with standard PWR dimensions and properties, except they are shorter in length. The proposed design is evaluated for deployment as a localized nuclear power station, providing 35 MWe via a once-through operation cycle (OTOC) of 5.5 years for self-sufficient carbon-free power supply.

The MINI-21 rector benefits from the availability and reliability of PWR components and expertise to leverage a reduction in costs associated with the UO_2 fuel cycle. A MINI-21 reactor can provide power for rural and remote locations, supporting agricultural, mining, and manufacturing type industries, or may be used to ensure grid stability as a dedicated power source for computer data centers, hospitals, communication centers, and community emergency hubs. The goal is to provide a robust contender for localized energy security needs as a stand-alone power supply or an integral member of a microgrid. This paper investigates the impact of incorporating proliferation-resistant fuel (PRF) [4,5]

into the MINI-21 design [6] for various reactor performance calculations, expanding upon previously presented work [7].

The increase in ^{238}Pu content in PRF can significantly reduce bomb yield due to its high spontaneous fission, and it contributes to high decay heat, which complicates the design and maintenance of explosive devices. An ideal goal would be to increase the ^{238}Pu/Pu isotopic ratio as much as possible to produce unfavorable plutonium fuel. However, greater ^{238}Pu/Pu ratios can also significantly complicate neutron shielding and decay heat mitigation for the transportation and storage of discharged nuclear fuel. Reduction in the ^{239}Pu/Pu isotopic ratio is another aspect of PRF. A balanced PRF compromise for the irradiated UO_2 fuel applied in this study is to (1) reduce the ^{239}Pu/Pu content to less than 90 wt.% and to (2) increase the ^{238}Pu/Pu content to greater than 2.5 wt.% [8]. The incorporation of minor actinides (MAs) such as Np, Am, and Cm in advanced nuclear fuel systems is promising [9], as these resources can be recycled or transmuted to less hazardous, or even more useful, forms rather than serving as increased waste stream considerations in expensive repository facilities. ^{237}Np can be transmuted and decayed into ^{238}Pu; the known disadvantages, however, are that there is a need to improve the transuranic cross section library data, and ^{237}Np is a controlled nuclear material.

Previous work has investigated the incorporation of ^{237}Np loadings in PRF to optimize the ability to meet the proposed requirements for a PWR for a nominal loading of 0.075 wt.% [10]. The optimization of the PRF content also included minimization of parasitic neutron absorption from the ^{237}Np additive [8]. This work investigates the performance of the MINI-21 design using a ^{237}Np loading of 0.075 wt.% in LEU+ UO_2 fuel via the verification-by-comparison (V-by-C) process in a series of Monte Carlo neutronics burnup analyses.

2. Materials and Methods

The MINI-21 FA includes 264 LEU+ (7.5 wt.% ^{235}U/U) UO_2 fuel rods, 24 control rod guide tubes, and one central guide tube for instrumentation. This previously presented core design [6] has a total fuel pin length of 135 cm and an 87.5 cm effective core outer diameter. Because of its small size, the initial UO_2 loading is ~4.1 t, compared to ~103 t in a typical PWR. A slightly higher enrichment than the traditional ~5 wt.% was selected for this design as it enabled a longer OTOC [11]. Currently, United States licensing limits are 5 wt.% ^{235}U enrichment and 62 GWd/t peak burnup, with near-term efforts to increase these limits to 8 wt.% and 75 GWd/t, respectively. Increased limits will allow for higher power density nuclear plants to extend fuel cycles up to 24 months in length, with positive economic savings [12]. SMRs can also benefit from increased fuel enrichment but will require additional measures of excess reactivity control to ensure safety and security coupled with extended operations.

Figure 1 provides an overview of the MINI-21 FA loading, including a 1/8th core model with two diagonal reflecting surfaces dissecting the core. The FAs are surrounded by regionally homogenized water and support structures. The model also accounts for axial and radial neutron leakage, which are important to account for in modeling small reactors. The FAs are arranged radially from the center, FA-0, to the outer limits of the core, FA-4. Table 1 shows a summary of some MINI-21 FA design parameters, and Figure 2 provides an overview of the FA layout.

Natural gadolinia, Gd_2O_3 (GdO), is used as the burnable absorber (BA) within the fuel to hold down initial excess reactivity and reduce the reactivity swing during operations to achieve a high-burnup fuel cycle. The BA loading pattern design for this LEU+ fuel is optimized to achieve three design goals for the MINI-21. First, the initial k_{eff} must be below 1.10. Second, the Δk swing band must be minimized as much as reasonably possible. Third, adequate excess reactivity must be available through the entire core operation cycle to achieve the desired burnup. These limits were selected to minimize the total control rod bank reactivity worth (7750 pcm bank limit). A radial grading strategy with enriched GdO BA has been previously demonstrated for SMR-21, -37, and -57 designs [6,13,14]. In the

MINI-21 design, a radial–axial grading approach is implemented by dividing the fuel pins in each FA into six axial fuel sections from L1 (top) to L6 (bottom), as depicted in Figure 1. Symmetrically, a reflecting boundary between L3 and L4 was implemented.

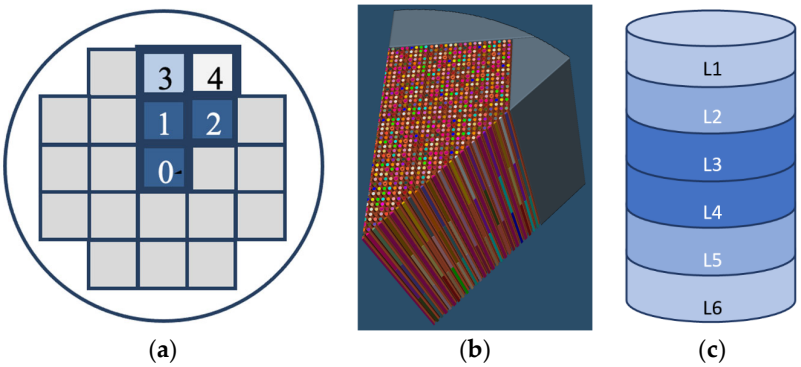
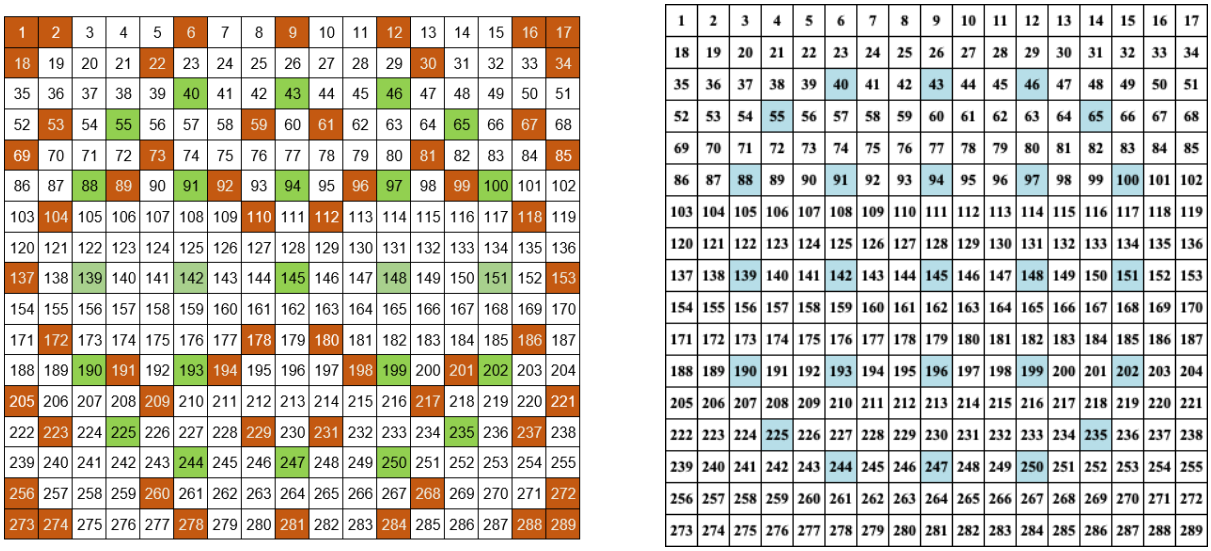


Figure 1. (**a**) MINI-21 fuel assembly loading, (**b**) 1/8th core model, (**c**) fuel pin axial zones.

This work utilizes a novel natural GdO BA loading design in using GdO BA homogenously mixed within all fuel pins for different axial loadings depending on the FA location within the reactor. Natural Gd consists of the isotopic vector provided in Table 2 [15]. Sensitivity studies were performed to determine the best axial–radial loading pattern design (see Table 3) to meet reactivity requirements. Previous efforts used enriched Gd mixed within only 56 fuel pins per assembly (as shown in Figure 2) [6]. From previous work, the typical loading pattern would include more BA in the central core regions and less in the outer regions. However, at the core center (FA-0 L3/L4) the fission power would be significantly depressed. Instead, the GdO BA content was reduced to zero, causing a donut-like loading pattern. There are five radial (FA-0 to FA-4) and three axial (L1/L6, L2/L5, and L3/L4) GdO BA loading zones. The BA is most heavily loaded in the central axial zones of FA-1 and FA-2. Standard fresh fuel without BA is loaded into many of the zones. There are two reactivity penalties associated with the use of a BA: the residual gadolinia will be discharged with the fuel at end of core life, and the initial reduction in uranium fuel loading. To maintain high-burnup fuel performance, an upper limit of 6.5 wt.% GdO was imposed in the design.

Table 1. MINI-21 17 × 17 fuel assembly design parameters.

Fuel assembly dimension	Square 21.5 cm × 21.5 cm
Positions per assembly	Total: 289 Fuel pins: 264 Control rod guide thimble: 24 Instrumentation thimble: 1 (center)
Fuel material	Uranium dioxide (UO_2)
Cladding material	Zircaloy-4
Gap filler	Helium gas
Fuel average density	95% theoretical density
Moderator (coolant)	Water at 0.72 g/cm^3
Enrichment	7.5 wt.% ^{235}U/U
Fuel pellet diameter	8.2 mm
Pellet–clad gap	0.082 mm
Clad thickness	0.572 mm
Fuel rod outer diameter	9.5 mm
Fuel rod length	135 cm



(**a**) (**b**)

Figure 2. (**a**) Original MINI-21 56-UGdO burnable absorber fuel pin arrangement (Adapted from [6]) vs. (**b**) current 17 × 17 fuel assembly uniformly loaded with natural burnable absorber in fuel pins.

Table 2. Natural isotopic abundances and thermal neutron capture cross sections for Gd [15].

Isotope	Abundance (at.%)	Cross Section (b)
^{152}Gd	0.20	700
^{154}Gd	2.18	60
^{155}Gd	14.80	61,000
^{156}Gd	20.47	2
^{157}Gd	15.65	255,000
^{158}Gd	24.84	2.4
^{160}Gd	21.86	1

Table 3. Radial and axial natural gadolinia burnable absorber loading (in wt.%).

Position	L1/L6 (Top/Bottom)	L2/L5	L3/L4 (Center)
FA-0	2.5	0	0
FA-1	0	4.5	6.5
FA-2	0	3.5	6.0
FA-3	0.1	0	0
FA-4	0	0	0

Four cases are evaluated via the V-by-C method. The base reference, Case A, uses 7.5 wt.% ^{235}U/U UO_2 fuel without inclusion of either ^{237}Np or GdO BA. Case B is Case A with the inclusion of 0.075 wt.% ^{237}Np in the fuel. Cases C and D modify Cases A and B to include the GdO BA loading from Table 1. Monte Carlo N-Particle® (MCNP®) version 5.1.40 [16] coupling with ORIGEN-2.2 [17] burnup BASH Script (MCOS) [18,19] was utilized to assess the OTOC for all four cases. MCNP serves as the transport solver, ORIGEN as the Bateman equation solver, and MCOS as the auto-linking transfer script between the two codes [20–22]. The MCNP 1/8th half-core 3D pin-by-pin working model with three axial fuel-pin layers has 2151 fuel node tallies.

The Evaluated Nuclear Data File, ENDF/B-VII.0 [23], is used in MCNP with the standard ORIGEN decay library data in ORIGEN. ORIGEN performs burnup calculations for MCOS using the matrix exponential method to calculate time-dependent formation,

destruction, and decay for each divided fuel cell. The neutron fission tally is proportional to the product of the fissile atomic density, fission cross sections, and the neutron flux tallies obtained from MCNP. The ORIGEN code with the IRP Specific Power Irradiation burnup calculation option was chosen in all the MCSO calculations, which can automatically adjust the neutron flux level to preserve the constant fission power during each burnup calculation time-step.

MCOS provides the following input parameters to ORIGEN: (1) the initial compositions and quantities of material, (2) one-group microscopic cross sections for each nuclide, (3) material feed and removal rates (if desired), (4) the length of the irradiation period(s), and (5) the flux or power. After each depletion/burnup calculation, ORIGEN reports quantities for 175 light materials, 141 actinides, and 1056 fission products with atomic densities greater than 1×10^{-12} atoms/b-cm into temporary files for the next time-step calculation. In this work, only the burnup-dependent one-group cross sections of nuclides whose reactions are criticality important are updated (see Table 4). The MCOS script will update the depleted isotopic compositions of each fuel material and send them back to MCNP for the next time-step burnup calculation. The multitasking nature of MCOS allows for a significant reduction in calculation time per time-step as only necessary information is redirected from the temporary data files. It should be noted that including the strong neutron absorbing fission products ^{135}Xe and ^{149}Sm will account for most of the fission product contribution to k_{eff}, which is sufficiently accurate for these calculations. When comparing computed results between depletion calculations including over 30 of the highest neutron-absorbing fission products against calculations only including ^{135}Xe and ^{149}Sm, the difference in k_{eff} is approximately 3.5%.

Table 4. Important radionuclides updated with each burnup step in MCOS.

Burnable Absorbers	^{154}Gd	^{155}Gd	^{156}Gd	^{157}Gd	^{158}Gd	^{160}Gd
Fission Products	^{135}Xe	^{149}Sm				
Actinides	^{235}U ^{240}Pu	^{238}U ^{241}Pu	^{237}Np ^{242}Pu	^{238}Np ^{241}Am	^{238}Pu ^{242}Am	^{239}Pu ^{242}Cm

3. Results and Discussion

3.1. Fuel Burnup Performance

The MCNP5 calculation for each MCOS time-step has 450 cycles with 3500 neutron particles sources (nps) apiece, representing a total of 1.575×10^6 total particles. The statistical uncertainty (1σ) is approximately 0.00065 in k_{eff}. The 1σ uncertainty in the 2151 fuel node tallies of the MCNP model is 1.12%. The uncertainties are considered adequately sufficient for the precision of the MCOS-calculated PRF OTOC performance analysis.

The calculated eigenvalue, k_{eff}, versus burnup for the four cases is plotted in Figure 3, showing the narrowed Δk reactivity swing band for Cases C and D. The initial k_{eff} values for Cases A through D are approximately 1.351, 1.342, 1.041, and 1.036, respectively. These values are lower than previously reported [7]. The general PWR startup to full power operation procedures are (1) Cold Shutdown (CS), (2) Cold Zero Power (CZP), (3) Hot Zero Power (HZP), (4) Hot Full Power (HFP) with no xenon, and (5) HFP with xenon equilibrium modes. Doppler effects were investigated similar to a previously calculated UO_2-fueled PWR [24]. At high burnup from 50 to 62 GWd/t, the MCOS-estimated Doppler coefficient is about 1.5 pcm (0.015 mk). The average fuel temperature at CZP and HZP are 300 K and 900 K, respectively. Therefore, the negative Doppler reactivity from CZP to HFP is approximately −900 pcm (−9 mk) in this work. Figure 3 shows that the ^{237}Np initial loading slightly reduces k_{eff} compared with those without, effectively demonstrating the excess reactivity reduction due to increased ^{237}Np inclusion. The reactivity penalty for ^{237}Np loading in Cases B and D compared against Cases A and C, respectively, is about

1000 pcm (10 mk). This penalty becomes negligible by the end of the OTOC. Case A k_{eff} decreases from 1.351 to 1.000 at a burnup of ~60 GWd/t. All other cases decrease to a k_{eff} of 1.000 between 59 and 63 GWd/t. There is no negative reactivity penalty from the inclusion of ^{237}Np and GdO BA on the OTOC when comparing Cases A and D.

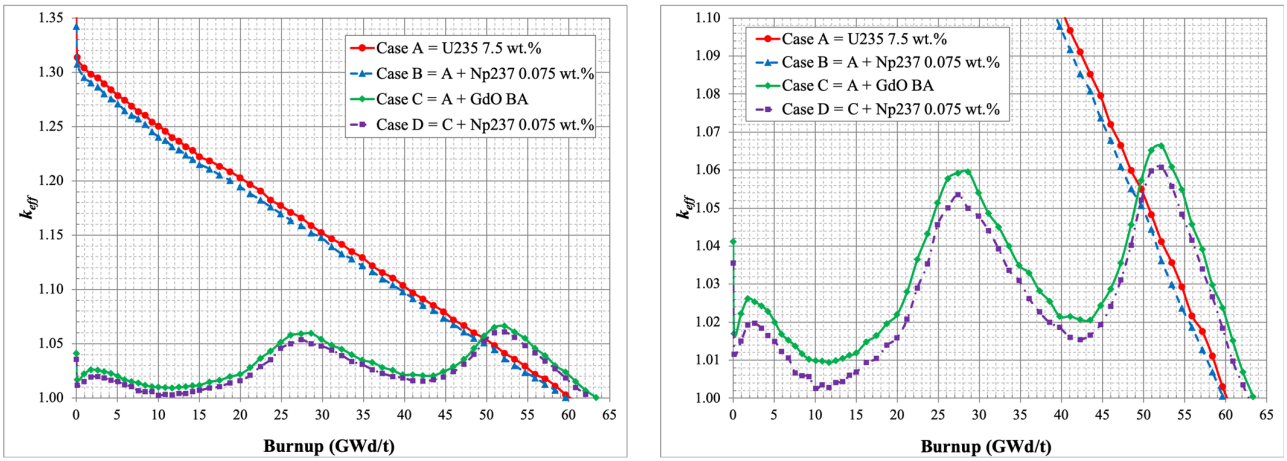


Figure 3. (**a**) Burnup-dependent k_{eff} for MINI-21, (**b**) closeup view of narrow reactivity band.

It is assumed that the total core power output is 35 MWe (112 MWt), which represents a fuel pin fission power density of ~283.4 W/cm^3. It will then take 5.5 years of full power operations to reach the discharge burnup. At the end of the core lifetime, a new prefabricated fresh fuel module can replace the discharged core, such that refueling and fuel-shuffling operations are not required for each OTOC core [25]. Cases C and D significantly reduce the initial core reactivity, more than the initial xenon equilibrium buildup, due to neutron self-shielding effects in the higher GdO BA loading. Variations in k_{eff} versus burnup increase slowly before dropping as the GdO is depleted from the various core regions. The average k_{eff} between 1 and 60 GWd is ~1.025, with a Δk reactivity swing (1σ) around this mean of ±0.016 (2.40$), which is proportionally small over the OTOC. The various peaks seen in Figure 3 for the k_{eff} of Cases C and D occur due to the depletion of GdO BA zones, burnup transition from the outer to inner zones of the cores, and ^{239}Pu buildup and depletion. Further discussion of how the fission power profile shifts with these changes is shown in Figure 4b.

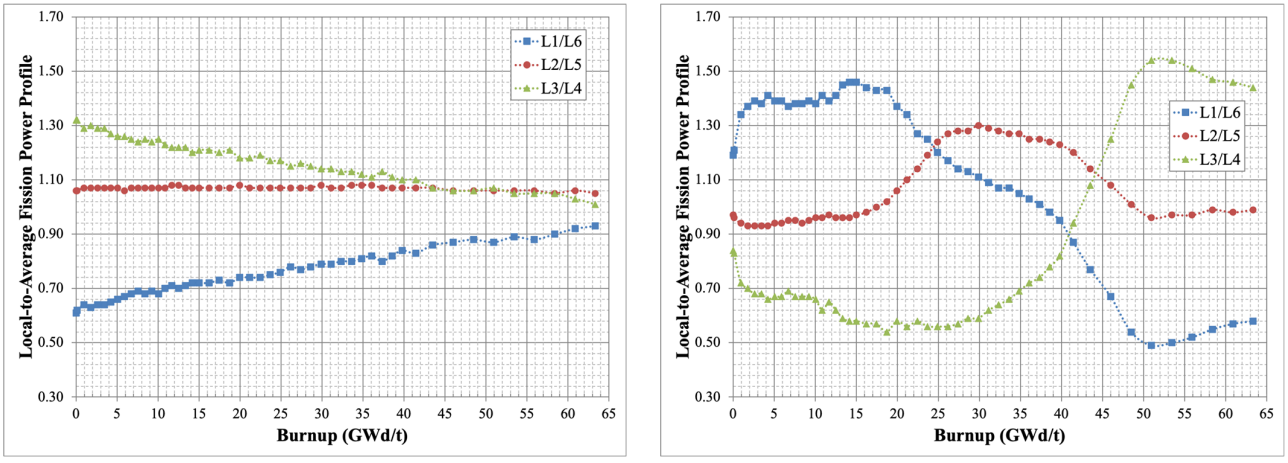


Figure 4. Radially averaged burnup-dependent local-to-average fission power ratios for (**a**) Case B and (**b**) Case D.

3.2. Fission Power Profile and Uranium Depletion

The axial profile of the FA-averaged local-to-average (L/A) fission power ratio is compared between Cases B and D at a burnup of 1.0 GWd/t (see Table 5). The addition of GdO BA in L3/L4 of FA-1 of Case D depresses the neutron flux, causing the L/A to drop from 1.53 to 0.20, as compared to Case B. The outer region (L1/L6 in FA-4) thus has an increased flux, and the L/A increases from 0.64 to 1.38. The radially averaged, burnup-dependent L/A ratio for Cases B and D is provided in Figure 4. For Case B, the peak L/A of ~1.30 occurs for L3/L4 at 1.0 GWd/t. The peak L/A value of ~1.52 does not occur for Case D until a burnup of ~52 GWd/t. Case B burns the fuel more heavily from the core center to the outer regions over the lifetime of the core. Case D burns from the outer region towards the center of the core.

Table 5. FA-averaged local-to-average fission power ratios at 1.0 GWd/t burnup.

Case B	**FA-0**	**FA-1**	**FA-2**	**FA-3**	**FA-4**	**Average**
L1/L6	0.63	0.63	0.64	0.64	0.64	0.64
L2/L5	1.53	1.27	1.10	0.79	0.65	1.07
L3/L4	1.84	1.53	1.32	0.64	0.77	1.28
Case D	**FA-0**	**FA-1**	**FA-2**	**FA-3**	**FA-4**	**Average**
L1/L6	0.55	1.52	1.60	1.63	1.38	1.34
L2/L5	0.86	0.40	0.44	1.62	1.39	0.94
L3/L4	0.53	0.20	0.24	1.40	1.21	0.72

The GdO BAs are loaded in the more power-peaking central regions, allowing for more fissile ^{235}U remaining in the central region of the core for the same burnup to 62.5 GWd/t. The result is that the core will have a larger un-depleted fraction (UDF) in the neutronically important central region for a net gain in excess reactivity over the core lifetime. Table 6 shows a comparison of UDF values between Cases B and D at a discharge burnup of 62.5 GWd/t. For region L3/L4 in FA-1, Case D has an increased ^{235}U UDF of 0.44 compared to 0.10 in Case B. There is a marginal decrease from 0.47 to 0.35 between Cases B and D for region L1/L6 in FA-4. The results confirm that the expected higher ^{235}U UDF in the central regions exists for a burnup of 62.5 GWd/t. The average UDF between Cases B and D are similar, with a slightly larger UDF in Case D with reduced content variability across the fuel assemblies. Burnup-dependent FA-averaged ^{235}U UDF values are plotted in Figure 5 for Cases B and D. A more efficient burnup of the fuel results in higher UDF values in Case D versus Case B, which also results in the slightly greater excess reactivity at core discharge, as seen in Figure 3.

Table 6. ^{235}U un-depleted fraction at 62.5 GWd/t burnup.

Case B	**L1/L6**	**L2/L5**	**L3/L4**	**Case D**	**L1/L6**	**L2/L5**	**L3/L4**
FA-0	0.19	0.08	0.06	FA-0	0.19	0.13	0.22
FA-1	0.25	0.12	0.10	FA-1	0.18	0.24	0.44
FA-2	0.29	0.16	0.13	FA-2	0.21	0.27	0.45
FA-3	0.40	0.25	0.21	FA-3	0.28	0.21	0.25
FA-4	0.47	0.32	0.28	FA-4	0.35	0.28	0.31
FA Ave.	0.32	0.19	0.16	FA Ave.	0.24	0.22	0.33
Core Ave.		0.22 ± 0.12		Core Ave.		0.27 ± 0.09	

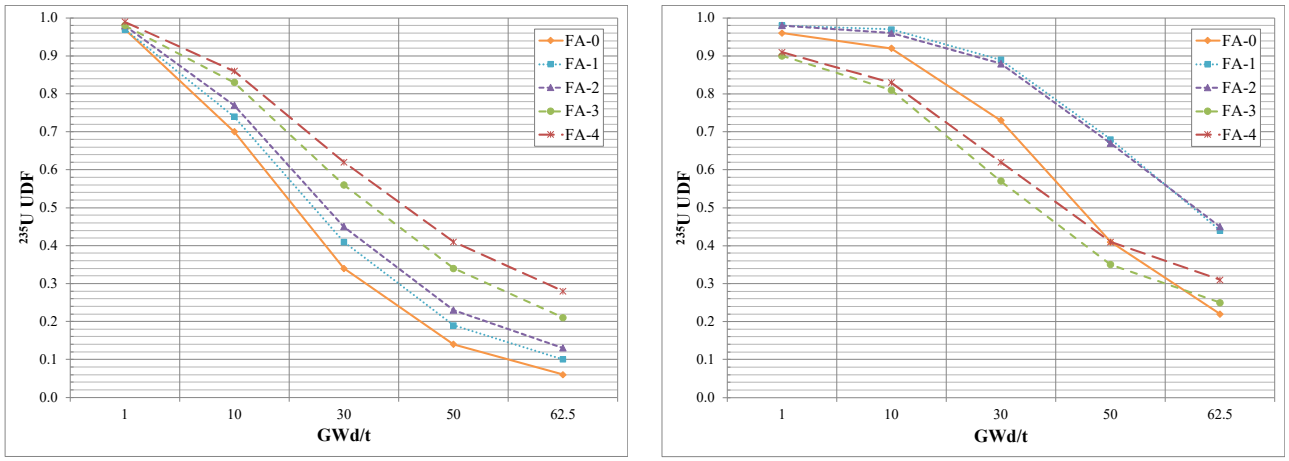


Figure 5. Assembly averaged burnup-dependent ^{235}U UDF at L3/L4 for (**a**) Case B and (**b**) Case D.

3.3. Burnable Adbsorber Depletion

Gadolinium has an extremely high thermal neutron absorption cross section, which will depress fuel pin power [26]. The depressed BA pins will increase the FA power peaking factor. To reduce this undesirable effect, the loading pattern in Table 1 was proposed as it limits power peaking while effectively holding down the initial core excess reactivity. Case D burnup-dependent ^{155}Gd and ^{157}Gd UDF profiles in FA-1 L3/L4 (6.5 wt.% GdO) depletion characteristics are plotted in Figure 6. As there is only a single fuel cycle in the MINI-21 design, the Gd is burned out at different rates depending on its location within the core. This figure shows the complete depletion of both ^{155}Gd and ^{157}Gd isotopes to a negligible UDF of ~0.075 wt.% at the discharge burnup of ~62.5 GWd/t. The reactivity penalty from the residual BA is negligible. Therefore, it can be concluded that the GdO BA design can achieve penalty-free core reactivity toward the discharge burnup.

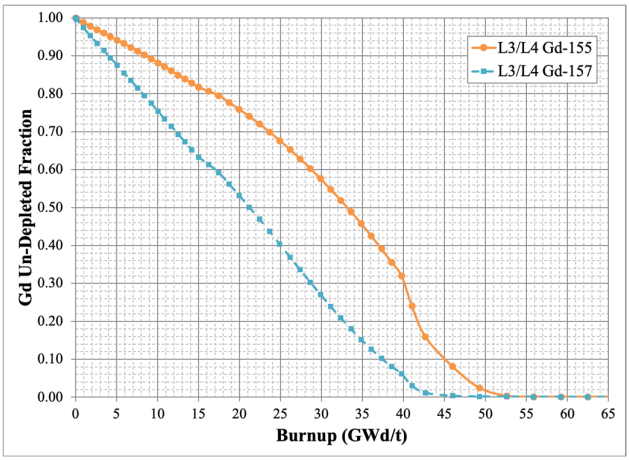


Figure 6. Gd un-depleted fraction versus burnup for Case D.

3.4. Neptunium and Plutonium Content

Aside from the initial contribution of ^{237}Np in Cases B and D, ^{237}Np and ^{238}Pu are produced during reactor operations via the following series of reactions:

$$^{235}\text{U} + \text{n} \rightarrow {}^{236}\text{U} + \text{n} \rightarrow {}^{237}\text{U} + \beta\ (6.75\ \text{d}) \rightarrow {}^{237}\text{Np} + \text{n} \rightarrow {}^{238}\text{Np} + \beta\ (2.1\ \text{d}) \rightarrow {}^{238}\text{Pu}.$$

The key reaction series producing ^{239}Pu is as follows:

$$^{238}\text{U} + \text{n} \rightarrow {}^{239}\text{U} + \beta\ (23\ \text{m}) \rightarrow {}^{239}\text{Np} + \beta\ (2.3\ \text{d}) \rightarrow {}^{239}\text{Pu}.$$

The core-averaged ^{237}Np content, in atomic density (a/b-cm), was calculated for all four cases, and is shown in Figure 7. The initial incorporation of 0.075 wt.% ^{237}Np within the fuel for Cases B and D start those cores out with an average content of 1.73×10^{-5} a/b-cm. The ^{237}Np content increases for all four cases with burnup. Case A increases from 0.0 to 4.01×10^{-6} a/b-cm, and Case D increases from 1.73×10^{-5} to 4.83×10^{-5} a/b-cm.

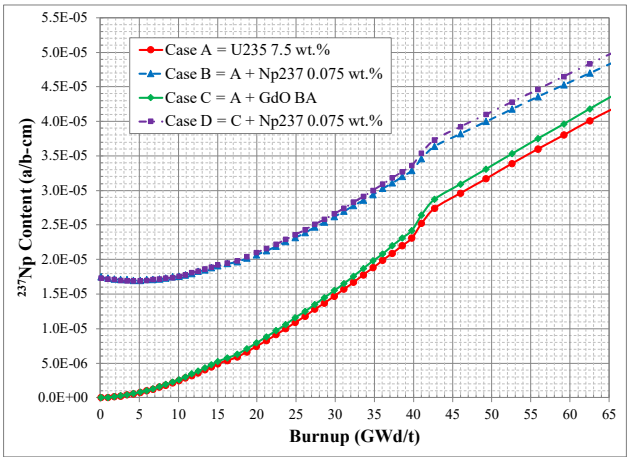


Figure 7. Core-averaged ^{237}Np content versus burnup.

The calculated core-averaged ^{238}Pu/Pu and ^{239}Pu/Pu isotopic ratios, as a function of burnup, are shown in Figure 8a,b, respectively. Due to the correlation between ^{237}Np and ^{238}Pu content, the trend is very similar between Figures 7 and 8a. The discharge ^{238}Pu/Pu ratios for Cases A through D are 6.05, 8.14, 5.90, and 8.01 wt.%, respectively. While the discharged fuel is above the lower threshold limit of 2.5 wt.% for all cases, only Cases B and D, which were initiated with some ^{237}Np content, are above this lower threshold limit throughout the entire core lifetime. To achieve this requirement for MINI-21, a core fuel loading of ~4.1 t would require a NpO_2 loading of ~3.1 kg. The results of isotopic profile calculations compare well with previously published works [9]. The ^{239}Pu/Pu ratios for all cases decrease from ~99 wt.% to below 90 wt.% within ~10 GWd/t of burnup. The concern that the lower burnup ratios are greater than 90 wt.%, which qualifies as weapons-grade Pu, is mitigated by the small total quantity of Pu produced at lower burnups (see Figure 9) and the short decay time of ^{238}Np when producing a high fraction of ^{238}Pu and providing increased proliferation resistance. Both Cases B and D satisfy the PRF requirements set in this study.

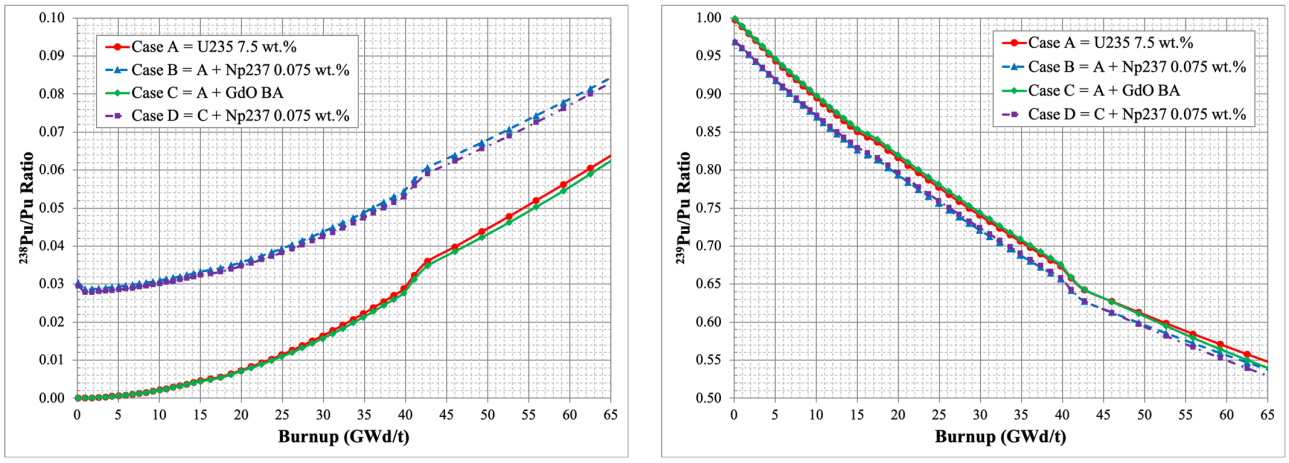
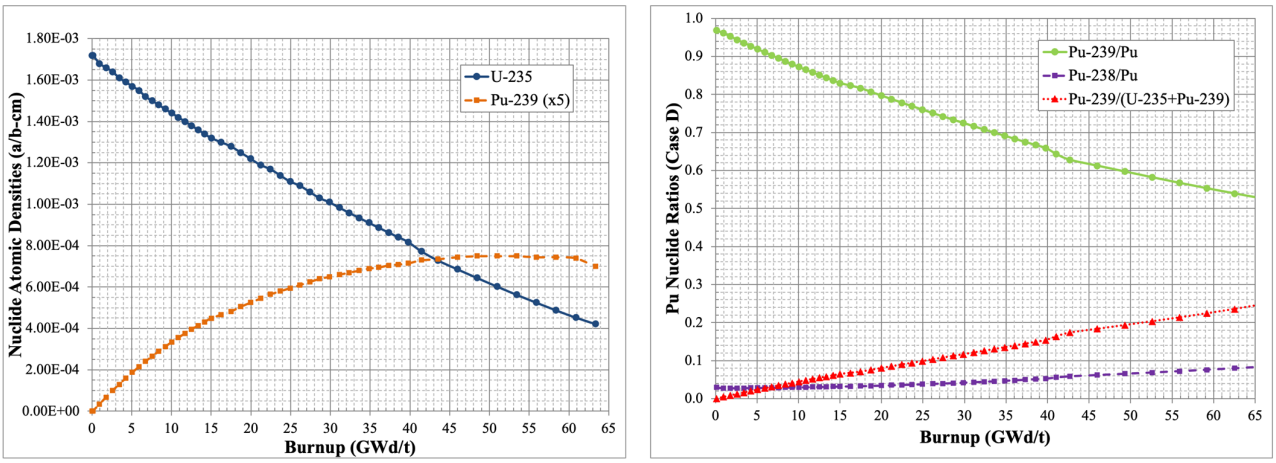


Figure 8. Core-averaged (**a**) ^{238}Pu/Pu and (**b**) ^{239}Pu/Pu isotopic ratio profiles, versus burnup.



(**a**) (**b**)

Figure 9. Core-averaged (**a**) U and Pu atomic densities and (**b**) Pu nuclide ratios, versus burnup.

Figure 9 provides an additional comparison between the Pu and U content of the fuel with burnup. The results provided are core-averaged. The ^{235}U atomic density steadily decreases from 1.72×10^{-3} a/b-cm to 4.22×10^{-4} a/b-cm by the end of the OTOC. The ^{239}Pu content peaks at 1.50×10^{-4} a/b-cm and then drops to 1.40×10^{-4} a/b-cm at core discharge. The ^{239}Pu/(^{235}U + ^{239}Pu) ratio is approximately 24% at the end of the OTOC, indicating that almost 1/4th of the power is produced by Pu at this point.

4. Conclusions

This study demonstrates that an OTOC for the MINI-21 reactor design is feasible for a ^{235}U enrichment of 7.5 wt.% up to a burnup of 62.5 GWd/t without the need for fuel reshuffling or onsite refueling. A 1/8th core model was utilized to evaluate four cases to understand the performance and impact of PRF and GdO BA loading within the fuel. The results demonstrate that the GdO BA loading can effectively hold down the initial excess reactivity with minimal penalties from reduced initial uranium content or residual gadolinia at core discharge; the reactivity swing during core lifetime operations can also be minimized. The inclusion of ^{237}Np satisfies the PRF goals of this study by quickly increasing the ^{238}Pu/Pu ratio to above 2.5 wt.% while also maintaining a reduced ^{239}Pu/Pu content over the core lifetime. Some key future investigational efforts include thermal–hydraulic and thermos–mechanical analyses of these fuels with core performance. The burnup-dependent Doppler coefficient of the MINI-21 design needs further detailed verification. Radial pin profiles to address rim effects and BA performance will also be investigated. The second phase of the MINI-21 design will incorporate these analyses with updated best available nuclear data to also investigate fuel storage pool design, as further detailed high-level spent fuel inventory evaluation would be necessary.

Author Contributions: Conceptualization, G.S.C., J.F., J.D.B. and P.M.; methodology, G.S.C.; software, G.S.C.; validation, G.S.C. and J.D.B.; formal analysis, G.S.C. and J.D.B.; investigation, G.S.C. and J.D.B.; resources, G.S.C. and J.F.; data curation, J.D.B. and G.S.C.; writing—original draft preparation, J.D.B. and G.S.C.; writing—review and editing, P.M. and J.F.; visualization, J.D.B. and G.S.C.; supervision, J.F.; project administration, J.F.; funding acquisition, J.F. All authors have read and agreed to the published version of the manuscript.

Funding: This research received no external funding.

Data Availability Statement: The datasets presented in this article are not readily available due to the proprietary nature of some of this research. Requests to access the datasets should be directed to Julie Foster (julie.foster@jfaidaho.com).

Conflicts of Interest: All authors were employed by the company JFoster & Associates, LLC. The authors declare that the research was conducted in the absence of any commercial or financial relationships that could be construed as a potential conflict of interest.

References

1. Virgili, N. *The Impact of Small Modular Reactors on Nuclear Non-Proliferation and IAEA Safeguards*; Vienna Center for Disarmament and Non-Proliferation: Vienna, Austria, 2020.
2. Godsey, K.M. Life Cycle Assessment of Small Modular Reactors Using U.S. Nuclear Fuel Cycle. Marster's Thesis, Environmental Health Physics, Clemson University, Clemson, SC, USA, 2019.
3. Mignacca, B.; Locatelli, G. Economics and Finance of Small Modular Reactors: A Systematic Review and Research Agenda. *Renew. Sust. Energy Rev.* **2020**, *118*, 109519. [CrossRef]
4. Chang, G.S. Enhancing PWR High Burnup Proliferation Resistance Fuel with Minor Actinides. *Trans. Am. Nucl. Soc.* **2007**, *96*, 759–762.
5. Chang, G.S. Enhancing BWR Proliferation Resistance Fuel with Minor Actinides. *J. Nucl. Mater.* **2009**, *385*, 157–160. [CrossRef]
6. Chang, G.; Foster, J.; Harrell, J. Mini-SMR-21 in Once-through Long-Lived Fuel Cycle Feasibility Assessment. *Trans. Am. Nucl. Soc.* **2020**, *122*, 675–678. [CrossRef]
7. Bess, J.D.; Chang, G.S.; Moo, P.; Foster, J. Verification of Mini-Reactor Minor-Actinide Proliferation Resistant Fuel with Burnable Gadolinia in Once-Through Operation Cycle Performance. In Proceedings of the PBNC 2024, Idaho Falls, ID, USA, 7–10 October 2024.
8. Serfontein, D.E.; Muldur, E.J.; Reitsma, F. Assessment and Reduction of Proliferation Risk Reactor-Grade Plutonium Regarding Construction of 'Fizzle Bombs' by Terrorist. *Nucl. Eng. Des.* **2014**, *271*, 545–551. [CrossRef]
9. Dodd, B.; Britt, T.; Lloyd, C.; Shah, M.; Goddard, B. Novel Homogeneous Burnable Poisons in Pressurized Water Reactor Ceramic Fuel. *Nucl. Eng. Technol.* **2020**, *52*, 2874–2879. [CrossRef]
10. Chang, G.S.; Bess, J.D.; Moo, P.; Hiruta, M.; Foster, J. PWR Minor Actinide Proliferation Resistant Fuel in Once-Through Fuel Cycle Performance Assessment. *Trans. Am. Nucl. Soc.* **2023**, *129*, 1004–1006.
11. Bess, J.D.; Chang, G.; Hiruta, M.; Foster, J. SMR LEU+ Very Long-Lived Once-through Fuel Cycle Spent Fuel Inventory Reduction Verification. In Proceedings of the WM2023, Phoenix, AZ, USA, 26 February–2 March 2023.
12. Lam, H.; Konig, A.; Wagener, C.; Franceschini, F. Westinghouse Advanced Fuel Management Strategies Leveraging High Enrichment and High Burnup Fuel to Optimize PWR Economics. In Proceedings of the PHYSOR 2022, Pittsburgh, PA, USA, 15–20 May 2022. [CrossRef]
13. Chang, G.; Foster, J.; Harrell, J. Validation of an SMR Gadolinia Burnable Absorber Loading Design with No-Onsite Refueling and Penalty-Free Reactivity. In Proceedings of the PHYSOR 2022, Pittsburgh, PA, USA, 15–20 May 2022. [CrossRef]
14. Chang, G.; Hiruta, M.; Foster, J.; Harrell, J. New Burnable Absorber Loading Design in SMR No-Onsite Refueling Strategy Performance Assessment. *Trans. Am. Nucl. Soc.* **2021**, *125*, 1049–1052.
15. Baum, E.M.; Ernesti, M.C.; Knox, H.D.; Miller, T.R.; Watson, A.M.; Travis, S.D. *Nuclides and Isotopes Chart of the Nuclides*, 17th ed.; Bechtel Marine Propulsion Corporation: Schenectady, NY, USA, 2010.
16. X-5 Monte Carlo Team. *MCNP—A General Monte Carlo N-Particle Transport Code, Version 5*; Volumes I (LA-UR-03-1987) and II (LA-CP-03-0245); [Revised 6/30/2004]; Los Alamos National Laboratory: Los Alamos, NM, USA, 2003.
17. Ludwig, S.B.; Croft, A.G. *To Manneschmidt, J. Letter Report, "Revision to ORIGEN2—Version 2.2"*; Oak Ridge National Laboratory: Oak Ridge, TN, USA, 2002.
18. Chang, G.S. Advanced CANDU Reactors Axial Xenon Oscillation Controllability Validation. *Ann. Nucl. Energy* **2016**, *96*, 441–445. [CrossRef]
19. Chang, G.S. PWR Advanced Fuel High Burnup-Dependent Xenon Oscillation Controllability Assessment. *Ann. Nucl. Energy* **2019**, *124*, 592–605. [CrossRef]
20. Chang, G.S.; Peterson, R.C. Burnup-Dependent Rim-Effect Comparison of WG-MOX Fuel Pellet in ATR and PWR. *Trans. Am. Nucl. Soc.* **2004**, *90*, 555–557.
21. Chang, G.S.; Peterson, R.C. Validation of Radial Power Profile in FRAPCON-3 by Monte-Carlo Method. *Trans. Am. Nucl. Soc.* **2001**, *85*, 385–386.
22. Chang, G.S.; Peterson, R.C. Weapons-Grade MOX Fuel Burnup Validation in ATR. *Trans. Am. Nucl. Soc.* **2001**, *84*, 239–240.
23. Chadwick, M.B.; Obložinský, P.; Herman, M.; Greene, N.M.; McKnight, R.D.; Smith, D.L.; Young, P.G.; MacFarlane, R.E.; Hale, G.M.; Frankle, S.C.; et al. ENDF/B-VII.0: Next Generation Evaluated Nuclear Data Library for Nuclear Science and Technology. *Nucl. Data Sheets* **2006**, *107*, 2931–3060. [CrossRef]
24. Kim, K.-O.; Jo, D. Analysis of Doppler Coefficients for Typical PWR UO_2 and MTR U_3Si_2-Al Fuels Using ENDF/B-VI and VII. *Ann. Nucl. Energy* **2015**, *85*, 1024–1028. [CrossRef]

25. Chang, G.; Foster, J.; Harrell, J. PWR Integral Gadolinia Burnable Absorber Loading Design in a Once-through Core Reactivity Swing Minimization Assessment. *Trans. Am. Nucl. Soc.* **2020**, *123*, 1419–1422. [CrossRef]
26. Brown, N.R.; Worrall, A.; Todosov, M. Impact of Thermal Spectrum Small Modular Reactors on Performance of Once-through Nuclear Fuel Cycles with Low-Enriched Uranium. *Ann. Nucl. Energy* **2017**, *101*, 166–173. [CrossRef]

Disclaimer/Publisher's Note: The statements, opinions and data contained in all publications are solely those of the individual author(s) and contributor(s) and not of MDPI and/or the editor(s). MDPI and/or the editor(s) disclaim responsibility for any injury to people or property resulting from any ideas, methods, instructions or products referred to in the content.